

$P - v$ criticalities, phase transitions and geometrothermodynamics of charged AdS black holes from Kaniadakis statistics

G. G. Luciano^{1,*} and E. N. Saridakis^{2,3,4,†}

¹*Applied Physics Section of Environmental Science Department, Escola Politècnica Superior, Universitat de Lleida, Av. Jaume II, 69, 25001 Lleida, Spain*

²*National Observatory of Athens, Lofos Nymfon, 11852 Athens, Greece*

³*CAS Key Laboratory for Researches in Galaxies and Cosmology, Department of Astronomy, University of Science and Technology of China, Hefei, Anhui 230026, P.R. China*

⁴*Departamento de Matemáticas, Universidad Católica del Norte, Avda. Angamos 0610, Casilla 1280 Antofagasta, Chile*

Boltzmann entropy-based thermodynamics of charged anti-de Sitter (AdS) black holes has been shown to exhibit physically interesting features, such as $P - V$ criticalities and van der Waals-like phase transitions. In this work we extend the study of these critical phenomena to Kaniadakis theory, which is a non-extensive generalization of the classical statistical mechanics incorporating relativity. By applying the typical framework of condensed-matter physics, we analyze the impact of Kaniadakis entropy onto the equation of state, the Gibbs free energy and the critical exponents of AdS black holes in the extended phase space. Additionally, we investigate the underlying microstructure of black holes in Ruppeiner geometry, which reveals appreciable deviations of the nature of the particle interactions from the standard behavior. Our analysis opens up new perspectives on the understanding of black hole thermodynamics in a relativistic statistical framework, highlighting the role of non-extensive corrections in the AdS black holes/van der Waals fluids dual picture.

I. INTRODUCTION

It is widely believed that black hole (BH) physics provides a promising arena to explore the quantum nature of gravity. After the pioneering discovery that BHs behave as thermodynamic systems [1, 2], the study of their properties has received a boost of new interest, and insights emerged toward the unification of general relativity, quantum theory and statistical physics [3, 4]. Yet, although BH dynamics can be fully described by a small number of classical parameters (namely mass, angular momentum and charge - *no hair theorem*), the microscopic degrees of freedom responsible for the thermal behavior of BHs have not yet been adequately identified [5].

The development of thermodynamic geometry (geometrothermodynamics) based on Weinhold [6] and Ruppeiner [7, 8] formalisms is an effort to extract, phenomenologically or qualitatively, the microscopic interaction information of a given system from the axioms of thermodynamics. The core idea is that, in ordinary thermodynamic systems, the curvature of Weinhold and Ruppeiner metrics is related to the nature of interactions among the underlying particles. For systems where the micro-structures interact attractively, the curvature scalar carries a negative sign, whereas it is positive for predominantly repulsive forces. Moreover, the metric is flat for non-interacting systems - such as the ideal gas - or systems where interactions are perfectly balanced. This scheme has been tested for a wide number of statistical physical models [8]. Interestingly enough, recent stud-

ies have revealed that it is feasible for BHs too [9–18], providing an empirical tool to access the microstructure of BHs from their macroscopic knowledge, despite the absence of a quantum gravitational theory.

Black holes in anti-de Sitter (AdS) spacetimes have been thoroughly studied in the last decades due to their applications in holography [19]. The observation that asymptotically AdS BHs can be described by dual thermal field theory has motivated a parallel study with condensed matter systems. This has led to the discovery of first order phase transitions in BHs [20–22] that resemble in many aspects the liquid-gas change of phase of van der Waals fluids [23–25]. A constitutive ingredient of this picture is the (negative) cosmological constant Λ , which is identified as pressure and included in the first law of BH thermodynamics alongside its conjugate quantity - the thermodynamic volume [26, 27]. The ensuing *extended phase space* allows to formulate the $P = P(V, T)$ equation of state and study the critical behavior of AdS BHs [27, 28].

A subtle concept in BH physics is thermodynamic entropy. According to the holographic principle [29, 30] BHs could store information at the event horizon like holograms. In the standard Boltzmann-Gibbs statistics, this behavior is encoded by the Bekenstein-Hawking area law, which states that BH entropy scales like the surface area

$$S_{BH} = \frac{A_{bh}}{A_0}, \quad (1)$$

where $A_0 = 4$ is the Planck area¹. Clearly, this is

*Electronic address: giuseppegaetano.luciano@udl.cat

†Electronic address: msaridak@noa.gr

¹ We adopt geometric units $\hbar = c = k_B = G = 1$.

an unconventional scaling. Indeed, if BHs are physically identified with their event horizon surface, then they can be regarded as genuine $(2+1)$ -dimensional systems and S_{BH} is with the correct (extensive) thermodynamic entropy. However, if BHs are to be considered as $(3+1)$ -dimensional objects (as arguably more natural in a $(3+1)$ -dimensional description of the spacetime background), then the area scaling would violate thermodynamic extensivity. Thus, Boltzmann-Gibbs theory may not be the appropriate framework for studying the thermodynamics of BHs, and a generalized non-additive entropy notion [31] or a quasi-homogeneous black hole thermodynamics [32] could be needed for such non-standard systems.

To better understand the intimate nature of BH entropy, several extensions of Boltzmann-Gibbs statistics have been considered in literature, motivated by either gravitational considerations (Tsallis [31, 33], Barrow [34] and more generalized [35] entropies) or information theory (Rényi [36] and Sharma-Mittal [37] entropies). Predictions of these models have been tested in cosmology [38–43] and quantum physics [44–47]. Recently, a non-extensive generalization inspired by the symmetries of the relativistic Lorentz group has been proposed by Kaniadakis [48–52] based on the modified entropy

$$S_\kappa = - \sum_i n_i \ln_\kappa n_i, \quad (2)$$

where the κ -deformed logarithm is defined by

$$\ln_\kappa x \equiv \frac{x^\kappa - x^{-\kappa}}{2\kappa}. \quad (3)$$

The generalized Boltzmann factor for the i -th microstate is

$$n_i = \alpha \exp_\kappa[-\beta(E_i - \mu)], \quad (4)$$

where

$$\exp_\kappa(x) \equiv \left(\sqrt{1 + \kappa^2 x^2} + \kappa x \right)^{1/\kappa}, \quad (5)$$

$$\alpha = [(1 - \kappa)/(1 + \kappa)]^{1/2\kappa}, \quad (6)$$

$$1/\beta = \sqrt{1 - \kappa^2} T, \quad (7)$$

with T and μ being the temperature and chemical potential of the system, respectively.

Deviations from Boltzmann-Gibbs statistics are quantified by the dimensionless parameter $-1 < \kappa < 1$. The classical framework is, however, recovered in the $\kappa \rightarrow 0$ limit. Besides theoretical arguments, we emphasize that phenomenological evidences for Kaniadakis statistics come from the high-quality agreement between the modified distribution (4) and the observed power-law tailed spectrum of cosmic rays [49].

One can show that, for the case of BHs, Kaniadakis entropy (2) can be cast as [53–57]

$$S_\kappa = \frac{1}{\kappa} \sinh(\kappa S_{BH}). \quad (8)$$

We mention here that, since the above expression is an even function of κ , i.e. $S_\kappa = S_{-\kappa}$, in the following we shall restrict to the $\kappa \geq 0$ domain.

Kaniadakis entropy in the form (8) has been mostly used for holographic applications and, in particular, to infer corrections brought about in the Friedmann equations [54–60] (see also [53] for a recent review). In the light of the gravity-thermodynamic conjecture, preliminary studies in BH thermodynamics have been considered in [61] by computing the κ -deformed temperature and heat capacity in the context of generalized Heisenberg relations [62, 63]. Nevertheless, to the best of our knowledge, a dedicated analysis of BH geometrothermodynamics and critical phenomena in Kaniadakis statistics has not yet been conducted.

Starting from the above premises, in this work we address the thermodynamics of AdS BHs from the Kaniadakis entropy perspective. We investigate the impact of Eq. (8) on small-large BH phase transitions and critical exponents by exploiting the language of condensed matter physics. In this sense, the main effort here is to lay the foundation towards formulating BH thermodynamics in a fully relativistic statistical context. We then examine the underlying microstructure of BHs in Ruppeiner geometry, which reveals predominantly repulsive intermolecular forces. In line with the discussion of [64–70], our analysis shows that the development of BH thermodynamics based on a non-extensive entropy notion involves a consistent redefinition of all other thermodynamic quantities, including the Hawking temperature and thermodynamic energy.

The structure of the work is as follows: for later comparison with physics of BHs, the next Section is devoted to review phase transitions and critical phenomena of van der Waals fluids. In Sec. III we study thermodynamics of charged AdS BHs in Kaniadakis statistics, while Sec. IV concerns geometrothermodynamic analysis. Conclusions and perspectives are finally discussed in Sec. V.

II. $P - V$ CRITICALITY OF VAN DER WAALS FLUIDS

Van der Waals model provides an effective description of real interacting fluids and liquid-gas phase transitions. The characteristic equation is

$$\left(P + \frac{a}{v^2}\right)(v - b) = T, \quad (9)$$

where $v = V/N$, N , V , P and T denote the specific volume, number of constituents, global volume, pressure and temperature of the van der Waals system, respectively. The positive constant a and b quantify the attraction and finite size of the molecules in the fluid.

The qualitative behavior of $P - V$ isotherms is displayed in Fig. 1. It can be seen that the *critical point* of the liquid-gas phase transition occurs when $P(v)$ has an

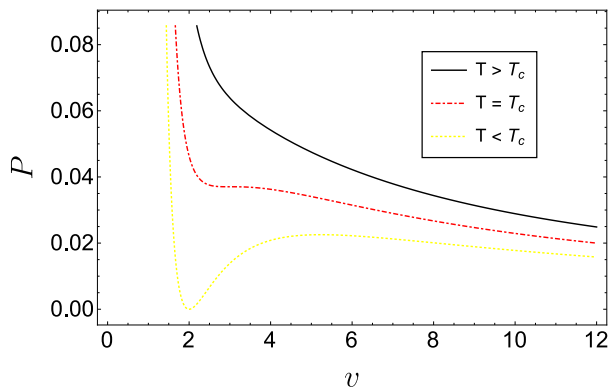


FIG. 1: $P - v$ diagram of van der Waals fluids. The red dot-dashed line indicates the critical isotherm at $T = T_c$. We have set $a = b = 1$ (online colors).

inflection point, which is obtained by imposing

$$\left(\frac{\partial P}{\partial v}\right)_T = \left(\frac{\partial^2 P}{\partial v^2}\right)_T = 0. \quad (10)$$

In this way, we obtain

$$v_c = 3b, \quad T_c = \frac{8a}{27b}, \quad P_c = \frac{a}{27b^2}, \quad (11)$$

for the critical volume, temperature and pressure, respectively. It is immediate to check that

$$P_c v_c / T_c = 3/8, \quad (12)$$

which is a universal number predicted for all fluids (independently of the constants a and b).

To gain more insights on the phase transitions of van der Waals fluids, let us introduce the (specific) Gibbs free energy, $G = G(P, T)$. For fixed N , this is given by [25]

$$G(T, P) = -T \left\{ 1 + \log \left[\frac{(v-b) T^{\frac{3}{2}}}{\lambda} \right] \right\} - \frac{a}{v} + Pv, \quad (13)$$

where v is to be understood as a function of pressure and temperature through Eq. (9), while λ is a (dimensional) specific constant of the gas. The behavior of G versus T is shown in Fig. 2 for different P . Below the critical pressure (yellow dotted curve), it exhibits the ‘‘swallowtail’’ shape characteristic of first order phase transitions from liquid to gas. Such a feature disappears for $P > P_c$ (black solid line).

The behavior of the physical variables near the critical point is quantitatively described by the critical exponents. Following [25], we introduce

$$t = \frac{T - T_c}{T_c} = \tau - 1, \quad \phi = \frac{v - v_c}{v_c} = \nu - 1. \quad (14)$$

The basic critical exponents α, β, γ and δ are then defined as follows (for computational details, see [71]):

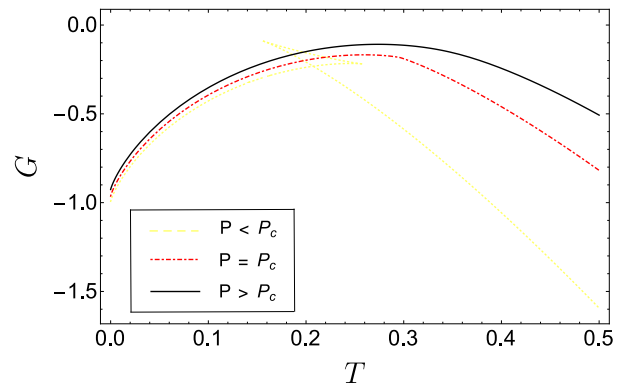


FIG. 2: Gibbs free energy G versus temperature T for various pressures P , for van der Waals fluids. The red dot-dashed line indicates the critical isobar at $P = P_c$ (online colors).

- α governs the dynamics of the specific heat at constant volume C_v according to $C_v = T \left(\frac{\partial S}{\partial T}\right)_v \propto |t|^{-\alpha}$. By explicit computation, one sees that C_v does not depend on t , which implies $\alpha = 0$.
- β describes the behavior of the order parameter $\eta = v_g - v_l$ for a given isotherm as $\eta \propto |t|^\beta$, where $v_{g,l}$ denote the volume of the gas and liquid phases, respectively. From the equation of corresponding states for van der Waals fluids and the Maxwell’s equal area law, it follows that $\beta = 1/2$.
- γ measures the isothermal compressibility κ_T of the fluid in compliance with $\kappa_T = -\frac{1}{v} \left(\frac{\partial v}{\partial P}\right)_T \propto |t|^{-\gamma}$. By using again the equation of corresponding states, one finds $\gamma = 1$.
- δ controls the difference $|P - P_c|$ on the critical isotherm $T = T_c$ according to $|P - P_c| \propto |v - v_c|^\delta$. The study of the shape of the critical isotherm gives $\delta = 3$.

The above considerations provide the basics of our next analysis. Specifically, we elaborate on the correspondence between phase transitions of BHs and van der Waals fluids within Kaniadakis framework, with focus on the κ -deformed analogues of Eq. (9)-(14).

III. KANIADAKIS THERMODYNAMICS OF CHARGED ADS BLACK HOLES

The general static and spherically symmetric metric that describes $(3 + 1)$ -dimensional charged AdS BHs in the Schwarzschild coordinates (t, r, θ, ϕ) is given by [72]

$$ds^2 = -f(r)dt^2 + f(r)^{-1}dr^2 + r^2 d\Omega^2, \quad (15)$$

where $d\Omega^2 = d\theta^2 + \sin^2\theta d\phi^2$ is the angular part of the metric on the two-sphere. Here, we have defined²

$$f(r) = 1 - \frac{2M}{r} + \frac{Q^2}{r^2} + \frac{r^2}{l^2}, \quad (16)$$

where M, Q are the mass and electric charge of the BH, respectively, while l is the AdS radius related to the (negative) cosmological constant by

$$\Lambda = -\frac{3}{l^2}. \quad (17)$$

In our setup, the parameter M shall be associated with the enthalpy of the BH conceived as a thermodynamic system. Clearly, for $Q = 0$ and $l \gg r$, Eq. (15) reduces to the well-known Schwarzschild metric. Additionally, the event horizon r_+ of the geometry (15) corresponds to the largest root of $f(r) = 0$. One can use this solution to express the BH mass as

$$M(r_+) = \frac{r_+}{2} + \frac{Q^2}{2r_+} + \frac{r_+^3}{2l^2}. \quad (18)$$

On the other hand, the surface area A_{bh} of the BH horizon reads

$$A_{bh} = \int_{r=r_+} \sqrt{g_{\theta\theta} g_{\phi\phi}} d\theta d\phi = 4\pi r_+^2. \quad (19)$$

Accordingly, the Boltzmann-Gibbs-based Bekenstein-Hawking entropy obeys the area law

$$S_{BH} = \frac{A_{bh}}{4} = \pi r_+^2. \quad (20)$$

As discussed in the Introduction, due to the area scaling of BH entropy, arguments from multiple perspectives suggest that Boltzmann-Gibbs statistics may not be the appropriate context for studying the thermodynamics of BHs. In particular, in a relativistic scenario Eq. (20) is expected to be generalized to Kaniadakis entropy (8), which we rewrite here by dropping for simplicity the index κ

$$S = \frac{1}{\kappa} \sinh(\kappa S_{BH}). \quad (21)$$

Two comments are in order: first, we observe that S is a monotonically increasing function of S_{BH} and, thus, of the horizon radius r_+ . Furthermore, in order to provide analytical solutions, it proves sometimes convenient to perform Taylor expansions for small κ [55, 78]. This

assumption is substantiated by the best agreement between theoretical predictions and phenomenological implications of Kaniadakis model, which is obtained for $\kappa = 0.2165$ in the physics of cosmic rays [49]. On the other hand, observational Cosmology constrains Kaniadakis parameter around zero [53], while the interval $0 < \kappa < 1$ has been considered in connection with the Bekenstein bound conjecture in Schwarzschild BHs [79]. In what follows, we shall retain the exact expression of S as far as possible, resorting to the small κ -approximation when strictly necessary.

The thermodynamic picture of AdS BHs is completed by the introduction of an extended phase space, where the pressure is identified with the cosmological constant and the thermodynamic volume with its conjugate quantity, i.e.

$$P = -\frac{\Lambda}{8\pi} = \frac{3}{8\pi l^2}, \quad (22)$$

$$V = \left(\frac{\partial M}{\partial P}\right)_{S,Q} = \frac{4}{3}\pi r_+^3, \quad (23)$$

respectively. Equipped with these new definitions, it is easy to check that BHs still obey the first law of thermodynamics [25]

$$dM = TdS + \varphi dQ + VdP, \quad (24)$$

and Smarr relation

$$M = 2(TS - VP) + \Phi Q, \quad (25)$$

where

$$T = \left(\frac{\partial M}{\partial S}\right)_{P,Q}, \quad \Phi = \left(\frac{\partial M}{\partial Q}\right)_{S,P}, \quad (26)$$

are the temperature and electric potential, respectively.

Using the standard thermodynamic machinery, we now have all the ingredients to compute the necessary BH thermodynamic variables. Since BH phase transitions have been shown to occur in the canonical (fixed charge) ensemble [20, 21], we conduct our analysis in this framework. As a first step, we express the mass parameter (18) in terms of the Kaniadakis entropy, using the relation (8). This gives

$$M(S) = \frac{(\pi l Q \kappa)^2 + \pi l^2 \kappa \operatorname{ash}(\kappa S) + \operatorname{ash}^2(\kappa S)}{2\pi^{\frac{3}{2}} l^2 \kappa^{\frac{3}{2}} \operatorname{ash}^{\frac{1}{2}}(\kappa S)}, \quad (27)$$

where we have introduced the shorthand notation

$$\operatorname{ash}(x) \equiv \operatorname{arcsinh}(x). \quad (28)$$

One can verify that the limit for $\kappa \rightarrow 0$ of Eq. (27) reproduces the standard expression of M for charged AdS BHs (solid black lines in Fig. 3), namely

$$M_{\kappa \rightarrow 0}(S) = \frac{S^2 + \pi l^2 (\pi Q^2 + S)}{2\pi^{\frac{3}{2}} l^2 S^{\frac{1}{2}}}. \quad (29)$$

² Following the study of [73–77] in Tsallis and Barrow frameworks, here we assume that Kaniadakis model only modifies BH entropy, while leaving the field equations of the theory unaffected. A comprehensive analysis of BH thermodynamics involving an ab initio derivation of a lagrangian driven by the Kaniadakis entropic index is reserved for the future.

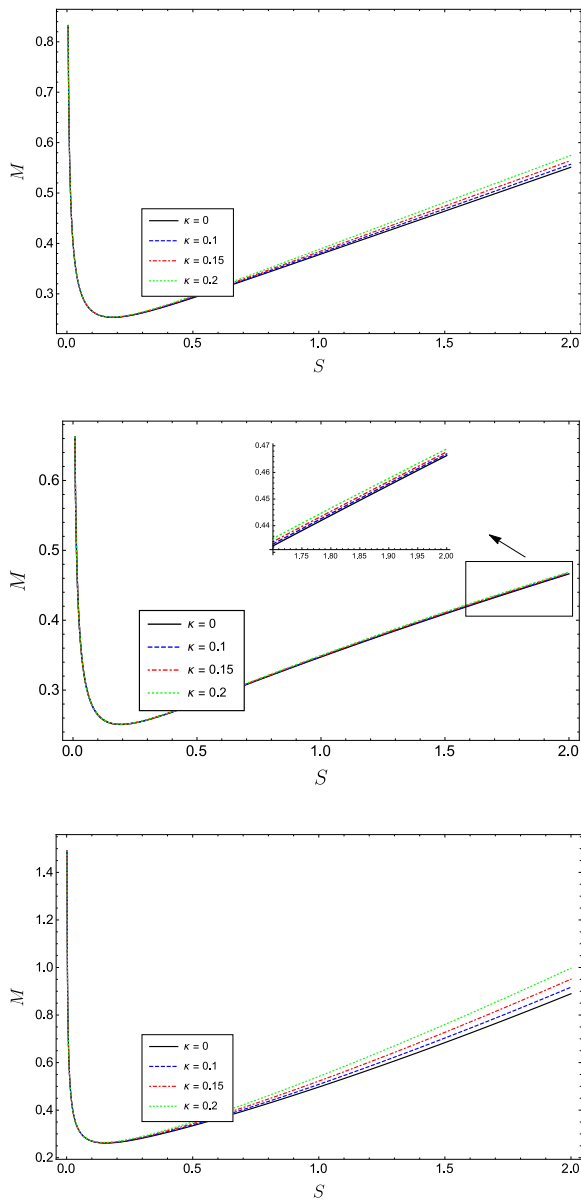


FIG. 3: The mass parameter M versus the entropy S for various values of κ , and for $l = l_c$ fixed through the critical condition (40) (upper panel), $l = 2l_c$ (middle panel) and $l = 0.5l_c$ (lower panel) (online colors).

The behavior of the κ -deformed mass (27) versus S is shown in Fig. 3 for various κ, l and fixed $Q = 0.25$ as in [80]. According to our previous considerations on the expected smallness of Kaniadakis exponent, we restrict to the range $\kappa \leq 0.2$. Note that in cosmological applications, κ is found to be much closer to zero [58, 59], however this does not need to be the case in BH applications (nevertheless, even in the present analysis one could use arbitrarily small values of the entropic parameter). As we can see, M remains positive and shows an initially decreasing behavior (evaporation phase of the BH), fol-

lowed by a later growth (absorption process). While leaving the initial stage of the evolution nearly unaffected, Kaniadakis entropy influences the final growth rate of M . In particular, the higher κ , the faster the growth, and vice-versa. For the sake of comparison with recent literature, we emphasize that a similar result has been found in the context of quantum gravity-induced deformations of Boltzmann-Gibbs entropy [75] and in non-linear electrodynamics and the Einstein-massive gravity [81].

The usage of Eq. (27) along with the first law of thermodynamics (24) allows us to derive the κ -temperature of the thermal radiation emitted by BHs as

$$T(S) = \left(\frac{\partial M}{\partial S} \right)_P \quad (30)$$

$$= \frac{-(\pi l Q \kappa)^2 + \pi l^2 \kappa \operatorname{ash}(\kappa S) + 3 \operatorname{ash}^2(\kappa S)}{4\pi^{\frac{3}{2}} l^2 [(1 + \kappa^2 S^2) \kappa \operatorname{ash}^3(\kappa S)]^{\frac{1}{2}}},$$

which, in the limit of $\kappa \rightarrow 0$, still recovers the usual result (solid black line in Fig. 4)

$$T_{\kappa \rightarrow 0}(S) = \frac{3S^2 + \pi l^2 (S - \pi Q^2)}{4\pi^{\frac{3}{2}} l^2 S^{\frac{3}{2}}}. \quad (31)$$

We further notice that the above relation has the well-defined Schwarzschild limit $T = 1/(4\pi r)$ for $Q \rightarrow 0$ and $l \rightarrow \infty$.

Equation (30) is plotted as a function of S in Fig. 4 for various κ, l and fixed Q as before. The points where the slope of the $T - S$ graphs vanishes are of special interest, as they signal a potentially critical behavior of BHs (see the next section for more quantitative discussion). From the upper and lower panel of Fig. 4, we observe that T increases monotonically and has one (upper panel) or no (lower panel) stationary point, depending on the value of l (or, equivalently, of P).

On the other hand, the middle panel shows that T increases for small (Region I - Small Black Hole (SBH)) and large (Region III - Large Black Hole (LBH)) values of the entropy, while it decreases in the intermediate domain (Region II - Intermediate Black Hole (IBH)). These regions are separated by two stationary points, which have been marked by vertical lines for better visual clarity. Effects of Kaniadakis entropy manifest through a variation of the width of the IBH region, with higher κ yielding a larger IBH domain and vice-versa. Below, we shall see this behavior of $T - S$ graph is peculiar to a first-order phase transition between SBH and LBH, which resembles in many aspects the liquid-gas change of phase of van der Waals fluids. In this picture, the larger amplitude of the IBH domain for higher κ can be understood in terms of the non-extensive character of Kaniadakis entropy by looking at the BH structure on a molecular level (see Sec. IV). For higher κ , indeed, the repulsive forces among BH microstructures tend to be weaker, at least in the first stage of BH evolution, which implies a slowed small-to-large phase transition of BH. To carry on the

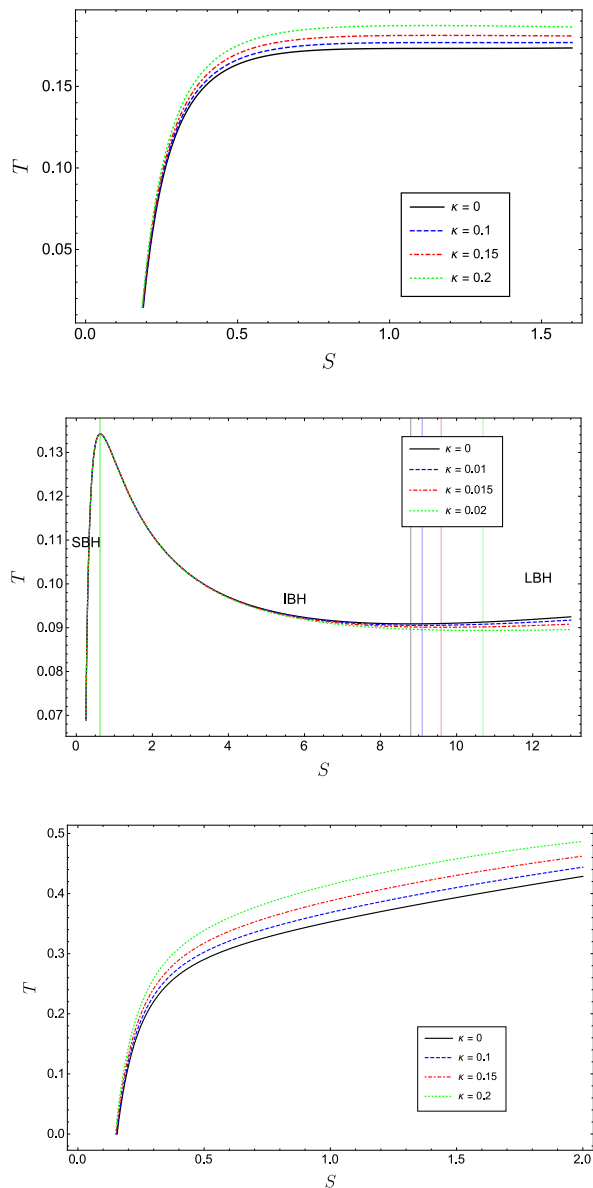


FIG. 4: The temperature T versus the entropy S for various values of κ , and for $l = l_c$ fixed through the critical condition (40) (upper panel), $l = 2l_c$ (middle panel) and $l = 0.5l_c$ (lower panel). In order to reveal all features of the $T - S$ diagrams, in the middle panel we have additionally considered smaller values of κ . The vertical lines in the middle panel separate Region II - Intermediate Black Hole (IBH) - from Region I - Small Black Hole (SBH) - and Region III - Large Black Hole (LBH) - see text (online colors).

similarity with van der Waals-like systems (where, however, interparticle forces are mostly attractive), one can think of a Kanidakis BH as a fluid with stronger attraction for larger κ . In this case, more heat is necessary to the internal molecules to overcome these attractive interactions, which results in a delayed liquid-gas change of phase.

Finally, regardless of the value of l , the condition $T(S_0) = 0$ gives the *physical limitation point of BHs*. Indeed, for $S < S_0$ the temperature becomes negative, which means this region is physically inaccessible.

Before moving on, we remark that the employment of generalized (non-extensive) entropies like that in Eq. (8) leads to multiplicity in the temperature value of BHs. In [68] it has been observed that three different scenarios may occur, depending on the assumed energy and temperature definitions. In compliance with [74, 75], here we are considering the energy definition of GR, the first law of thermodynamics and the thermodynamic temperature definition as fundamental. An alternative viewpoint has been adopted in [68], based on the assumption that the Hawking temperature must be kept unaffected. It is interesting to explore whether, and if so, how the present results get modified in such a complementary approach. Investigation along this direction is left for future work.

A. Heat capacity and critical point

With the help of the temperature (30), one can obtain the heat capacity at constant pressure as

$$\begin{aligned}
C_p(S) = T \left(\frac{\partial S}{\partial T} \right)_P &= -\frac{2}{\kappa} (1 + \kappa^2 S^2)^{\frac{3}{2}} \operatorname{ash}(\kappa S) \left[(\pi l Q \kappa)^2 - \operatorname{ash}(\kappa S) (\pi l^2 \kappa + 3 \operatorname{ash}(\kappa S)) \right] \\
&\times \left\{ 3 (\pi l Q \kappa)^2 (1 + \kappa^2 S^2) - \operatorname{ash}(\kappa S) \left\{ \pi l^2 \kappa \left[1 + \kappa^2 S \left(S - 2\pi Q^2 (1 + \kappa^2 S^2)^{\frac{1}{2}} \right) \right] \right. \right. \\
&\left. \left. + \operatorname{ash}(\kappa S) \left[-3 + \kappa^2 S \left(-3S + 2\pi l^2 (1 + \kappa^2 S^2)^{\frac{1}{2}} \right) + 6\kappa S \operatorname{ash}(\kappa S) (1 + \kappa^2 S^2)^{\frac{1}{2}} \right] \right\} \right\}^{-1}, \quad (32)
\end{aligned}$$

which for $\kappa \rightarrow 0$ consistently reduces to (solid black line in Fig. 5)

$$C_{p,\kappa \rightarrow 0}(S) = \frac{2S [3S^2 + \pi l^2 (S - \pi Q^2)]}{\pi l^2 (3\pi Q^2 - S) + 3S^2}. \quad (33)$$

It is important to note that $C_p > 0$ corresponds to local stability of BHs, while for $C_p < 0$ even small perturbations may cause BH disappearance. Also, discontinuities potentially indicate a critical behavior of BHs.

Equation (32) is plotted as a function of S in Fig. 5 for various κ, l and fixed Q as before. In compliance with the discussion below Eq. (30), it is observed that C_p has one (upper panel), two (middle panel) or no (lower panel) discontinuity, depending on the value of l . The SBH, IBH and LBH regions are clearly distinguishable from the middle panel (the vertical lines correspond to the two stationary points of the $T - S$ graphs in the middle panel of Fig. 4). While SBH and LBH are thermodynamically stable ($C_p > 0$), IBH is unstable ($C_p < 0$). As discussed, for instance, in [25] this gives rise to a transition between the SBH and LBH “phases”. As l progressively decreases to a certain critical value (upper panel), the IMB range reduces to a point, which in turn corresponds to the single stationary point of the $T - S$ graph in the upper panel of Fig. 4. By further decreasing l (lower panel), C_p is always continuous and keeps positive values. In this case, BHs are locally stable and do not undergo any transition (see also the corresponding $T - S$ graphs in the lower panel of Fig. 4).

To better understand the origin of this critical value of l , we now derive the analogue of the equation of state (9) for BHs in the extended phase space. By using Eq. (22) and (30), after some algebra we get

$$P(r_+) = \cosh(\pi \kappa r_+^2) \frac{T}{2r_+} + \frac{Q^2}{8\pi r_+^4} - \frac{1}{8\pi r_+^2}, \quad (34)$$

which is now straightforward to match with the $\kappa \rightarrow 0$ limit [25]

$$P_{\kappa \rightarrow 0}(r_+) = \frac{T}{2r_+} + \frac{Q^2}{8\pi r_+^4} - \frac{1}{8\pi r_+^2}. \quad (35)$$

To directly compare Eq. (34) with Eq. (9), let us identify the horizon radius r_+ with the specific volume of van

der Waals fluid as [25]

$$v = 2r_+. \quad (36)$$

In this way, we obtain

$$P(v) = \cosh\left(\frac{\pi \kappa v^2}{4}\right) \frac{T}{v} + \frac{2Q^2}{\pi v^4} - \frac{1}{2\pi v^2}. \quad (37)$$

As discussed for van der Waals fluids, the critical point of phase transitions can be derived from the conditions (10). However, analytical expressions for the critical specific volume, temperature and pressure can only be obtained to the leading order in κ . In this approximation, we are allowed to write down

$$v_c = 2\sqrt{6}Q + 144\sqrt{6}\pi^2 Q^5 \kappa^2 + \mathcal{O}(\kappa^3), \quad (38)$$

$$T_c = \frac{1}{3\sqrt{6}\pi Q} + 3\sqrt{6}\pi Q^3 \kappa^2 + \mathcal{O}(\kappa^3), \quad (39)$$

$$P_c = \frac{1}{96\pi Q^2} + 2\pi Q^2 \kappa^2 + \mathcal{O}(\kappa^3), \quad l_c^2 = \frac{3}{8\pi P_c}, \quad (40)$$

all reducing to the standard critical expressions for $\kappa \rightarrow 0$ [25].

From Eq. (38), we can also infer the thermodynamic volume corresponding to the critical volume v_c , which is

$$\begin{aligned}
V_c &= \left(\frac{\partial M}{\partial P} \right)_S \Big|_{r_+=r_c} = \frac{4}{3} \pi r_c^3 \\
&= 8\sqrt{6}\pi Q^3 + 1728\sqrt{6}\pi^3 Q^7 \kappa^2 + \mathcal{O}(\kappa^3). \quad (41)
\end{aligned}$$

It is worth noting that $v_c \rightarrow 0$, while $T_c, P_c \rightarrow \infty$ for $Q \rightarrow 0$ regardless of κ , which means that the critical transition described above is characteristic of charged BHs also in Kaniadakis entropy model (on the other hand, in [82] it has been found that AdS BHs in Gauss-Bonnet gravity undergo small-large transitions in the uncharged case too).

Interestingly enough, the critical parameters (38)-(40) satisfy the relation

$$\frac{P_c v_c}{T_c} = \frac{3}{8} + \frac{315}{4} \pi^2 Q^4 \kappa^2 + \mathcal{O}(\kappa^3). \quad (42)$$

By comparison with Eq. (12), we see that Kaniadakis entropy-based BHs slightly deviate from pure van der

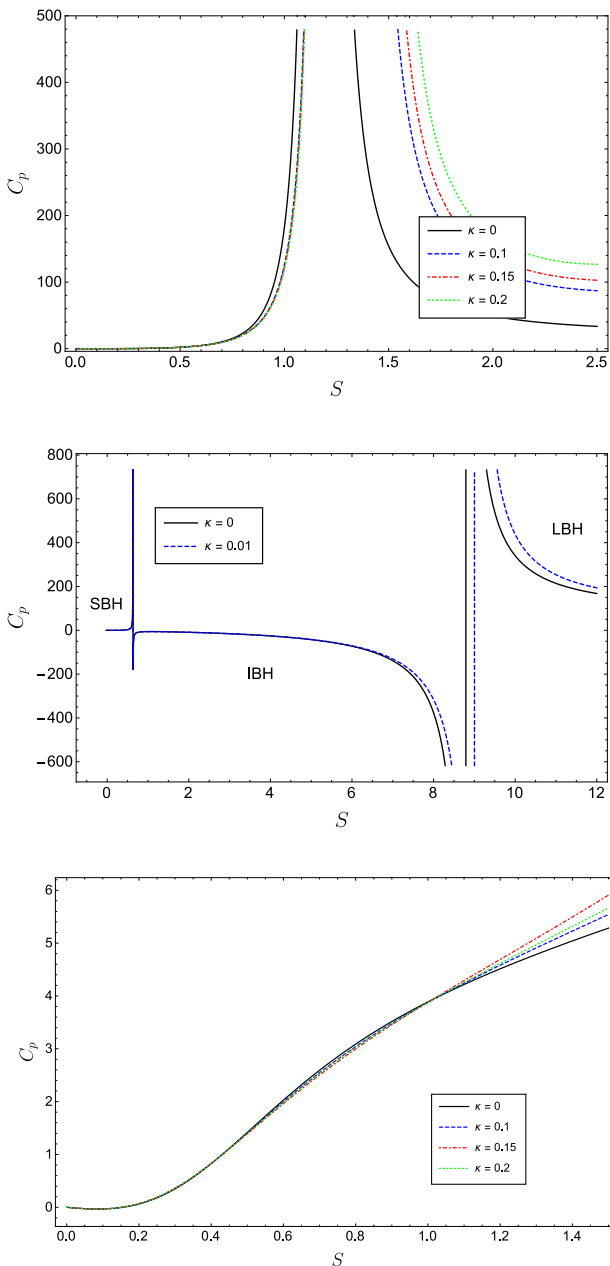


FIG. 5: The heat capacity at constant pressure C_p versus the entropy S for various κ values, and for $l = l_c$ fixed through the critical condition (40) (upper panel), $l = 2l_c$ (middle panel) and $l = 0.5l_c$ (lower panel). For visual clarity, we have only considered two values of κ in the middle panel (online colors).

Waal behavior, due to the κ -dependent correction. The latter behavior is, however, recovered for $\kappa \rightarrow 0$.

Now, by introducing the re-scaled variables

$$p = \frac{P}{P_c}, \quad \nu = \frac{v}{v_c}, \quad \tau = \frac{T}{T_c}, \quad (43)$$

the equation of state (37) can be rearranged as

$$8\tau = 3\nu \left(Ap + \frac{2B}{\nu^2} \right) - \frac{D}{\nu^3}, \quad (44)$$

where

$$A = \frac{8P_c v_c}{3T_c \cosh\left(\frac{\pi\kappa v^2}{4}\right)} = 1 + 6\pi^2 Q^4 (35 - 3\nu^4) \kappa^2 + \mathcal{O}(\kappa^3), \quad (45)$$

$$B = \frac{2}{3\pi T_c v_c \cosh\left(\frac{\pi\kappa v^2}{4}\right)} = 1 - 18\pi^2 Q^4 (7 + \nu^4) \kappa^2 + \mathcal{O}(\kappa^3) \quad (46)$$

$$D = \frac{16Q^2}{\pi T_c v_c^3 \cosh\left(\frac{\pi\kappa v^2}{4}\right)} = 1 - 18\pi^2 Q^4 (15 + \nu^4) \kappa^2 + \mathcal{O}(\kappa^3). \quad (47)$$

Equation (44) has the same structure as the law of corresponding states for fluids [25]

$$8\tau = 3\nu \left(p + \frac{2}{\nu^2} \right) - \frac{1}{\nu^3}. \quad (48)$$

It is easy to check that this equation is correctly restored for $\kappa \rightarrow 0$, since $A = B = D = 1$ in this limit.

B. $P - v$ diagram

We proceed by investigating the $P - v$ diagrams of AdS BHs as given in Eq. (37). These diagrams are displayed in Fig. 6 for various κ , T and fixed Q as before. By comparison with Fig. 1, we see that the isotherms at $T < T_c$ (green and yellow curves) have van der Waals-like oscillations with a local minimum and maximum. As T increases to T_c (red curve), the oscillating branch squeezes and the two stationary points converge into the inflection point (P_c, v_c, T_c) (see Eqs. (38)-(40)). This behaviour is reminiscent of the van der Waals fluid transition. Though not changing the qualitative behavior of the isotherms, Kaniadakis entropy non-trivially affects the critical pressure and temperature at which such transition occurs. For $T > T_c$ (blue and black curves), there are no more stationary points and P decreases monotonically along each isotherm.

C. Gibbs free energy

Let us now explore the global stability of charged AdS BHs in Kaniadakis thermodynamics. For this purpose,

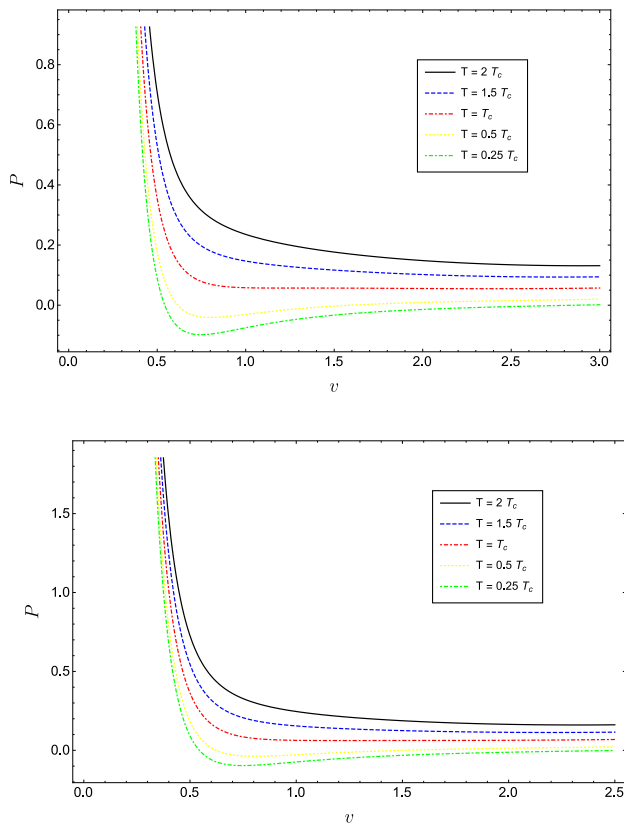


FIG. 6: $P - v$ diagrams for $\kappa = 0.1$ (top panel) and $\kappa = 0.15$ (bottom panel). In each panel, the temperature of the isotherms decreases from top to bottom. The red dot-dashed line indicates the critical isotherm at $T = T_c$ (online colors).

we compute the Gibbs free energy as [25, 83]

$$G(T, P) = M - TS = \frac{3(Q^2 + r_+^2) + 8\pi P r_+^4}{6r_+} \quad (49)$$

$$+ \frac{[Q^2 - r_+^2(1 + 8\pi P r_+^2)]}{4\pi\kappa r_+^3} \tanh(\pi\kappa r_+^2),$$

where r_+ is to be regarded as a function of P and T through the equation of state (34). Once more, one can check that the $\kappa \rightarrow 0$ limit gives back the classical Gibbs free energy for charged AdS BHs

$$G_{\kappa \rightarrow 0}(T, P) = \frac{3Q^2}{4r_+} + \frac{r_+}{4} - \frac{2}{3}\pi P r_+^3. \quad (50)$$

The behavior of Eq. (49) as a function of T is shown in Fig. 7, to be compared with Fig. 2. Consistently with the previous discussion, it is observed that, below the critical pressure (dotted yellow line), G exhibits the swallow tail behavior typical of first order phase transitions. Specifically, in the first branch BHs are in the SBH domain. As T increases to the critical point O , SBH and LBH phases coexist, since they have the same Gibbs free energy. As noted in [25], the coexistence line in the $P - T$

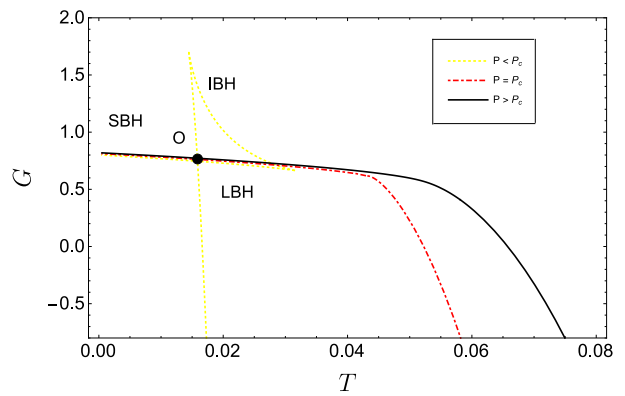


FIG. 7: The Gibbs free energy G versus the temperature T , for $\kappa = 0.1$ (the same qualitative behavior is obtained for other values of κ). The red dot-dashed line indicates the critical isobar at $P = P_c$. SBH denotes Region I - Small Black Hole, IBH denotes Region II - Intermediate Black Hole and LBH denotes Region III - Large Black Hole, see text (online colors).

plane can be derived by using Maxwell's equal area law or finding a curve for which G and T coincide for SBH and LBH. This line is plainly visible from the 3D plot in Fig. 8. Above the critical temperature, LBH becomes the preferred thermodynamic state because of its lower Gibbs free energy. Therefore, there is a first-order small-large phase transition at the point O . Clearly, owing to the definition (8) of entropy, different horizon areas for the SBH and LBH during this transition correspond to a discontinuity in the entropy (and also in the thermodynamic volume, see Eq. (23)) and, thus, to the release of latent heat.

D. Behavior near the critical point

For quantitative discussion of the behavior of BHs approaching the critical point, we now calculate the critical parameters as defined at the end of Sec. II. First, we introduce the free energy

$$F(T, V) = G - PV. \quad (51)$$

By using Eqs. (23) and (49), we get

$$F = \frac{1}{2} \left[\frac{Q^2}{r_+} + r_+ - \frac{2T \sinh(\pi\kappa r_+^2)}{\kappa} \right]. \quad (52)$$

Accordingly, the entropy is

$$S(T, V) = - \left(\frac{\partial F}{\partial T} \right)_V = \frac{\sinh(\pi\kappa r_+^2)}{\kappa}, \quad (53)$$

consistently with Eq. (8). In turn, from the definition below Eq. (14), we find that $C_V = 0$, which yields $\alpha = 0$.

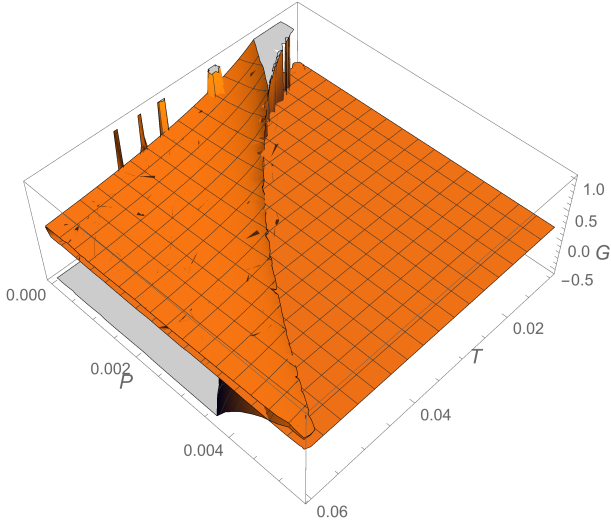


FIG. 8: 3D plot of the Gibbs free energy G versus pressure P and temperature T , for $\kappa = 0.1$ (the same qualitative behavior can be obtained for other values of κ). The coexistence line between the SBH and LBH phases in the $P - T$ plane is visible.

In order to compute β , we approximate Eq. (44) around a critical point. We use the re-scaled coordinates (14), here rewritten for convenience as

$$t = \frac{T}{T_c} - 1, \quad \omega = \frac{V}{V_c} - 1. \quad (54)$$

In the approximation of small κ , we obtain

$$p = 1 + \left(\frac{8}{3} - 512\pi^2 Q^4 \kappa^2\right) t + \left(-\frac{8}{3} + 704\pi^2 Q^4 \kappa^2\right) t\omega + \left(-\frac{4}{3} + 1120\pi^2 Q^4 \kappa^2\right) \omega^3 + \mathcal{O}(t\omega^2, \omega^4), \quad (55)$$

where the various terms have been grouped together in this specific way for a direct comparison with [25]. It is worth noting that the re-scaled pressure as appears in Eq. (55) contains terms of order higher than the quadratic in κ , due to the implicit κ -dependence of t, ω . However, for our purpose of computing Kaniadakis corrections to critical exponents, it is useful to present Eq. (55) et seq. in their current form and restore the leading order at the end. For more details on the validity of the series expansion respect to t, ω , see [25].

Now, differentiation of Eq. (55) respect to ω at a fixed $t < 0$ gives

$$dp = P_c \left[\left(-\frac{8}{3} + 704\pi^2 Q^4 \kappa^2\right) t + (-4 + 3360\pi^2 Q^4 \kappa^2) \omega^2 \right] d\omega. \quad (56)$$

By employing Maxwell's equal area law

$$\oint v dP = 0, \quad (57)$$

along with the knowledge that there is no pressure variation during the phase transition, we obtain

$$\begin{aligned} & 1 + \left(\frac{8}{3} - 512\pi^2 Q^4 \kappa^2\right) t + \left(-\frac{8}{3} + 704\pi^2 Q^4 \kappa^2\right) t\omega_l + \left(-\frac{4}{3} + 1120\pi^2 Q^4 \kappa^2\right) \omega_l^3 \\ & = 1 + \left(\frac{8}{3} - 512\pi^2 Q^4 \kappa^2\right) t + \left(-\frac{8}{3} + 704\pi^2 Q^4 \kappa^2\right) t\omega_s + \left(-\frac{4}{3} + 1120\pi^2 Q^4 \kappa^2\right) \omega_s^3 \end{aligned} \quad (58)$$

and

$$0 = \int_{\omega_l}^{\omega_s} \omega \left[\left(-\frac{8}{3} + 704\pi^2 Q^4 \kappa^2\right) t + (-4 + 3360\pi^2 Q^4 \kappa^2) \omega^2 \right] d\omega, \quad (59)$$

where $\omega_{s,l}$ denote the “specific volume” of the small and large phases of BHs, respectively. One can verify that the only non-vanishing solution that reduces to the standard

one for $\kappa \rightarrow 0$ is [25]

$$\omega_s = -\omega_l = \sqrt{-2t} (1 + 288\pi^2 Q^4 \kappa^2). \quad (60)$$

Thus, from the definition of the critical exponent β below

Eq. (14), it follows that

$$\eta = V_c(\omega_l - \omega_s) = 2V_c\omega_l \propto \sqrt{-t} \implies \beta = \frac{1}{2}. \quad (61)$$

As concerns the exponent γ , we need to differentiate Eq. (55) as

$$\left(\frac{dV}{dP}\right)_T = \frac{V_c}{P_c} \left(\frac{d\omega}{dp}\right)_T = -\frac{3}{8} \frac{V_c}{P_c} \frac{1}{t} (1 + 264\pi^2 Q^4 \kappa^2). \quad (62)$$

Hence, the isotherm compressibility κ_T of BHs takes the form

$$\kappa_T = -\frac{1}{V} \left(\frac{\partial V}{\partial P}\right)_T \propto \frac{1}{t}, \quad (63)$$

which implies $\gamma = 1$.

Lastly, the shape of the critical isotherm $t = 0$ and the related δ -exponent are given by

$$p - 1 = \left(-\frac{4}{3} + 1120\pi^2 Q^4 \kappa^2\right) \omega^3 \implies \delta = 3. \quad (64)$$

In spite of the non-trivial modifications induced by the κ -deformed entropy to the critical pressure, volume and temperature, the basic critical exponents remain unaffected. This allows to conclude that the qualitative similarity between Kaniadakis BHs and van der Waals fluids near the critical point holds at quantitative level too.

E. Sparsity of black hole radiation

Although BHs nearly behave like a black body and spontaneously emit particles at a temperature proportional to their surface gravity, the flow of Hawking radiation exhibits some peculiar features. For instance, it is known to be more sparse than black body radiation. Quantitatively speaking, such a difference can be estimated through the computation of the so-called sparsity, which is a measure of the average time-gap between the emission of successive quanta defined by

$$\tilde{\eta} = \frac{C}{g} \left(\frac{\lambda_t^2}{A_{eff}}\right), \quad (65)$$

(we have used the symbol $\tilde{\eta}$ instead of the traditional η to avoid confusion with the critical exponent (61)). Here, the constant C is dimensionless, while g , $\lambda_t = 2\pi/T$ and $A_{eff} = 27A_{bh}/4$ denote the spin degeneracy factor of the emitted quanta, the thermal wavelength and the effective horizon area of the BH, respectively. For Schwarzschild BHs and emission of massless bosons, one has $\lambda_t = 2\pi/T_H = 8\pi^2 r_h$, which entails

$$\tilde{\eta}_H = \frac{64\pi^3}{27} \approx 73.49 \gg 1. \quad (66)$$

For comparison, we remind that $\tilde{\eta} \ll 1$ in the case of a black body.

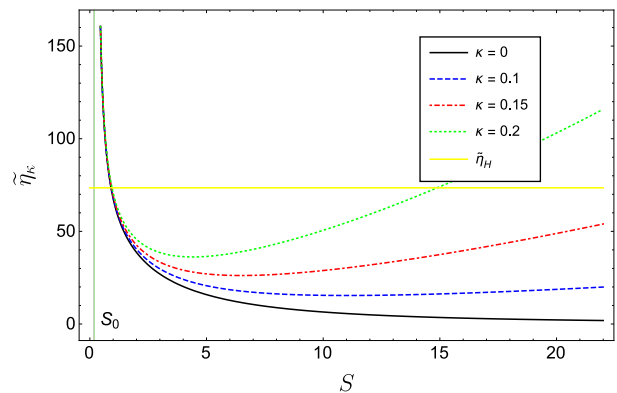


FIG. 9: The sparsity $\tilde{\eta}_\kappa$ versus the entropy S , for various κ and $l = 2$. The vertical lines represent the physical limitation entropy S_0 for each curve. For comparison, we have also depicted the sparsity of Schwarzschild BHs with emission of massless bosons (yellow curve) (online colors).

Effects of deformed entropies on sparsity of Schwarzschild BHs have been recently considered in literature (see [61, 84–86] and references therein). For instance, in [61] it has been shown that generalized models of Heisenberg relation combined with non-extensive (Rényi, Tsallis-Cirto, Kaniadakis, Sharma Mittal and Barrow) entropies lead to substantial modifications of the sparsity, which turns out to be mass dependent. A similar statement has been claimed in [86] in rainbow gravity. The question arises as to how such results appear for charged AdS BHs in Kaniadakis framework.

To compute the κ -deformed sparsity, we resort to the definition (65) equipped with Eq. (30). Straightforward calculations yield

$$\tilde{\eta}_\kappa = \tilde{\eta}_H \frac{\pi^2 l^4 \kappa^2 (1 + \kappa^2 S^2) \text{ash}^2(\kappa S)}{\left[-(\pi l Q \kappa)^2 + \pi l^2 \kappa \text{ash}(\kappa S) + 3 \text{ash}^2(\kappa S)\right]^2}. \quad (67)$$

We notice that in the Schwarzschild limit (i.e. $Q = 0$ and sufficiently large AdS radius l), this expression reduces to

$$\tilde{\eta}_\kappa(Q = 0, l \rightarrow \infty) = \tilde{\eta}_H (1 + \kappa^2 S^2), \quad (68)$$

which coincides with the result of [61] for Schwarzschild BHs. By further imposing $\kappa \rightarrow 0$, we have $\tilde{\eta}_\kappa = \tilde{\eta}_H$, as expected.

The behavior of the κ -modified sparsity (67) for various κ and fixed $l = 2$, $Q = 0.25$ is plotted in Fig. 9, which shows an apparent divergence for a certain (κ -dependent) value of S . This singularity, however, lies at the physical limitation point S_0 (see the discussion below Eq. (30)), as it is easy to understand from the definition (65). Thus, it is unphysical and we only have to consider the region $S > S_0$ delimited by the vertical line. We can see that the κ -deformed sparsity lies always above the $\kappa = 0$ (black) curve, in such a way that increasing the value of κ directly results in sparser Kaniadakis BH radiation. This

is in line with the result of [61]. On the other hand, $\tilde{\eta}_\kappa$ is greater than the sparsity $\tilde{\eta}_H$ of Hawking radiation of Schwarzschild BHs (yellow curve) for sufficiently small and large entropies, where it significantly departs from the black body-like behavior, while it falls below in the intermediate range.

IV. GEOMETROTHERMODYNAMICS OF CHARGED ADS BLACK HOLES

Since it is possible to define a temperature for BHs, it is natural to think of an associated substructure. Recently, special care has been devoted to analyze the microscopic constituents and underlying interactions of BHs [9–18], which can be described in the same fashion as the molecules of a non-ideal fluid.

To investigate phenomenologically the nature of interactions among BH microstructures, the common technique consists in studying the thermodynamic geometry of the whole macroscopic system. In this perspective, the analysis of Weinhold [6] and Ruppeiner [7, 8] geometries has proved to give qualitative insights on the internal dynamics of ordinary thermodynamics systems via exploring the sign of the corresponding metric curvature. Specifically, negative (positive) scalar curvatures emerge for prevailing attractive (repulsive) microinteractions, while flatness characterizes non-interacting systems, such as the ideal gas, or systems where interactions are perfectly balanced.

In the effort to probe the character of BH microinteractions, Weinhold and Ruppeiner formalisms have been adapted to BH thermodynamics. This kind of study has been first developed for Banados, Teitelboim and Zanelli (BTZ) BHs [9] and later extended to Reissner-Nordström, Kerr and Reissner-Nordström-AdS BHs [87]. In the plethora of results obtained so far, there is general consensus that the scalar curvature of BH systems with charged molecules should be positive, revealing a repulsive behavior of microinteractions [10–12, 14].

In order to figure out to what extent Kaniadakis' prescription (8) affects the above conclusion, let us compute Weinhold and Ruppeiner scalar curvature in Kaniadakis entropy-based thermodynamics. Toward this end, we remind that Weinhold metric is defined as the second derivative of internal energy of the system with respect to given thermodynamic variables [6]. For the case of BHs, by identifying the internal energy with the mass, we obtain

$$g_{ij}^w = -\partial_i \partial_j M(S, P, Q) \implies ds_w^2 = g_{ij}^w dx^i dx^j, \quad (69)$$

where we have we have generically denoted the independent fluctuation coordinates by x^i .

Similarly, in Ruppeiner formalism one considers the entropy as basic thermodynamic potential, i.e.

$$g_{ij}^{Rup} = -\partial_i \partial_j S. \quad (70)$$

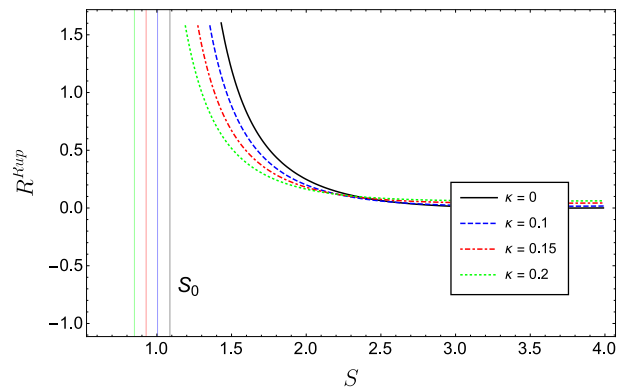


FIG. 10: The Ruppeiner scalar curvature R^{Rup} versus the entropy S , for various values of κ . The parameter l is fixed to $l = \sqrt{2}l_c$ defined through the critical condition (40). The vertical lines represent the physical limitation entropy S_0 for each curve (online colors).

From Eqs. (30), (69) and (70), it follows that the line elements of Weinhold and Ruppeiner are connected each other via the conformal transformation [88]

$$ds_R^2 = \frac{ds_w^2}{T}. \quad (71)$$

We focus our next geometrothermodynamic analysis on Eq. (71). Considering the entropy and pressure as the fluctuation coordinates, while keeping Q fixed, we obtain the following expression for the Ruppeiner scalar curvature:

$$\begin{aligned} R^{Rup}(S, P) &= (1 + \kappa^2 S^2)^{-\frac{1}{2}} [\text{ash}(\kappa S)]^{-1} \\ &\quad \times \kappa^2 [-2\pi Q^2 \kappa + \text{ash}(\kappa S)] \\ &\quad \times \left\{ \pi (Q\kappa)^2 - \text{ash}(\kappa S) [\kappa + 8P \text{ash}(\kappa S)] \right\}^{-1} \end{aligned} \quad (72)$$

which reduces to the standard curvature for charged AdS BHs in the $\kappa \rightarrow 0$ limit [12]

$$R_{\kappa \rightarrow 0}^{Rup}(S, P) = \frac{2\pi Q^2 - S}{S[-\pi Q^2 + S(1 + 8PS)]}. \quad (73)$$

The curvature (72) versus S is displayed in Fig. 10 for various κ and fixed $Q = 0.6$, $P = 0.5P_c$. As discussed for the sparsity above, the physical region is delimited by $S > S_0$ (vertical lines). Although Eq. (72) is non-trivially modified comparing to the classical curvature (73), Kaniadakis entropy does not affect the overall sign of R^{Rup} , which is still positive and indicates prevailing repulsive interactions among BH microstructures. As S increases, R^{Rup} gradually decreases, which means that the repulsion progressively fades, possibly due to thermal fluctuations and/or molecular collisions. Kaniadakis corrections here manifest through a variation of the rate of decrease, with higher κ corresponding to

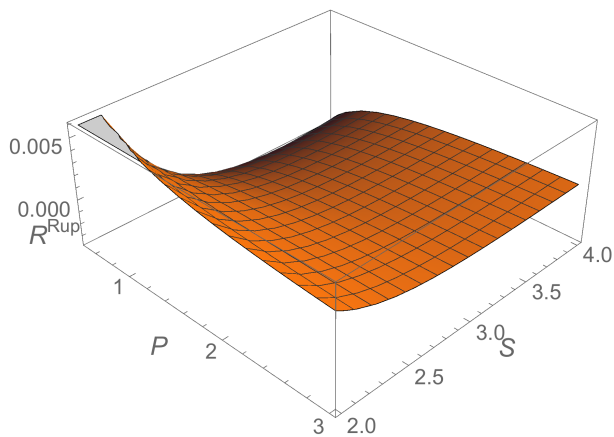


FIG. 11: 3D plot of the Ruppeiner scalar curvature R^{Rup} versus entropy S and pressure P , for $\kappa = 0.2$ and $Q = 0.6$.

faster decrease for sufficiently small S , and vice-versa. This tendency is reversed for S large enough. The former behavior resembles the physics of composite systems with non-extensive (and, in particular, superadditive) entropy. Indeed, for such systems the single constituents tend to merge more strongly than the classical extensive case [89], thus balancing swiftly the effects of internal repulsive forces. Asymptotically (i.e. for large BH horizon radii), the internal microstructures end up being so far apart that $R^{Rup} \rightarrow 0$, which reveals that BHs behave as effectively non-interacting.

Finally, Fig. 11 shows the 3D plot of R^{Rup} versus S and P for $\kappa = 0.2$ and fixed Q as before. We can see that the scalar curvature remains positive even for varying P , which supports previous arguments on the repulsive nature of BH micro-interactions.

V. CONCLUSIONS AND DISCUSSION

Geometrothermodynamics and phase transitions of charged AdS BHs have been addressed within the framework of Kaniadakis theory, which arises from a self-consistent relativistic generalization of the classical statistical mechanics. The latter is coherently recovered by setting the deformation parameter κ to zero. We would like to stress that the highlight of the present analysis is to deepen our knowledge of BH thermodynamics in a fully relativistic statistical scenario. As far as we know, this is the first work where this scenario is addressed.

Following the standard literature, the study has been conducted by identifying the cosmological constant and its conjugate quantity with the thermodynamic pressure and volume, respectively. In the ensuing extended phase space, we have examined the impact of Kaniadakis en-

tropy on the formal duality black-hole/fluid, showing that Kaniadakis BHs still exhibit a van der Waals-like first order phase transition.

Although Kaniadakis corrections do not affect the qualitative behavior of $P-v$ diagrams and the basic critical exponents, the critical volume, pressure and temperature are non-trivially modified, even at the leading order in the deformation parameter κ (see Eqs. (38)-(40)). Should we have access to the phenomenology of AdS BHs and measure such quantities, we could elaborate more on the role of Kaniadakis entropy in BH physics and possibly constrain κ -corrections. We have finally probed the nature of interactions among BH micro-structures. Using the picture of fluid-like interacting molecules, we have applied Ruppeiner geometrothermodynamic formalism and computed the scalar curvature of the associated metric. The investigation of the sign of the Ruppeiner scalar curvature R^{Rup} reveals that these micro-interactions are prevailing repulsive and tend to vanish for sufficiently large BH horizon radii, with the κ -parameter ruling the rate of decrease. In passing, we mention that a possible explanation for this behavior can be provided based on the physics of the two fluid model, where the dominant character of interactions is determined by the relative number densities of the molecules of the two fluids [12].

As future prospects, it would be interesting to enrich the above analysis by considering the presence of global monopoles, which are known to have non-trivial effects on BH physics [90–94]. Furthermore, one can study Kaniadakis entropy-based thermodynamics of other BHs, such as rotating or exotic BTZ BHs, and additionally examine its effect on the primordial black holes and stochastic gravitational waves [95, 96]. On the other hand, inspired by [61], it is suggestive to understand how BH critical phenomena appear in the context of modified uncertainty principles [97, 98] combined with nonextensive entropies, and possibly connect the two frameworks. The study of these aspects is under active consideration and will be presented elsewhere.

Acknowledgments

GGL would like to thank Jaume Giné for useful comments on the original manuscript. He is also grateful to the Spanish “Ministerio de Universidades” for the awarded Maria Zambrano fellowship and funding received from the European Union - NextGenerationEU. The authors acknowledge the contribution of the LISA CosWG and of COST Actions CA18108 “Quantum Gravity Phenomenology in the multi-messenger approach” and CA21136 “Addressing observational tensions in cosmology with systematics and fundamental physics (CosmoVerse)”.

- [1] S. W. Hawking, *Commun. Math. Phys.* **43**, 199 (1975) [erratum: *Commun. Math. Phys.* **46**, 206 (1976)].
- [2] J. D. Bekenstein, *Phys. Rev. D* **7**, 2333 (1973).
- [3] J.M. Bardeen, B. Carter, and S. Hawking, *Commun. Math. Phys.* **31**, 161 (1973).
- [4] S. W. Hawking and D. N. Page, *Commun. Math. Phys.* **87**, 577 (1983).
- [5] R. M. Wald, *Living Rev. Rel.* **4**, 6 (2001).
- [6] F. Weinhold, *J. Chem. Phys.* **63**, 2479 (1975).
- [7] G. Ruppeiner, *Phys. Rev. A* **20**, 1608 (1979).
- [8] G. Ruppeiner, *Rev. Mod. Phys.* **67**, 605659 (1995).
- [9] R. G. Cai and J. H. Cho, *Phys. Rev. D* **60**, 067502 (1999).
- [10] S. W. Wei and Y. X. Liu, *Phys. Rev. Lett.* **115**, 111302 (2015) [erratum: *Phys. Rev. Lett.* **116**, 169903 (2016)].
- [11] S. W. Wei, Y. X. Liu and R. B. Mann, *Phys. Rev. Lett.* **123**, 071103 (2019).
- [12] X. Y. Guo, H. F. Li, L. C. Zhang and R. Zhao, *Phys. Rev. D* **100**, 064036 (2019).
- [13] Z. M. Xu, B. Wu and W. L. Yang, *Phys. Rev. D* **101**, 024018 (2020).
- [14] A. Ghosh and C. Bhamidipati, *Phys. Rev. D* **101**, 106007 (2020).
- [15] Z. M. Xu, B. Wu and W. L. Yang, *Eur. Phys. J. C* **80**, 997 (2020).
- [16] E. Hirunsirisawat, R. Nakarachinda and C. Promsiri, *Phys. Rev. D* **105**, 124049 (2022).
- [17] A. Dehghani, B. Pourhassan, S. Zarepour and E. N. Saridakis, [arXiv:2305.08219 [hep-th]].
- [18] F. F. Santos, B. Pourhassan and E. Saridakis, [arXiv:2305.05794 [hep-th]].
- [19] E. Witten, *Adv. Theor. Math. Phys.* **2**, 253 (1998).
- [20] A. Chamblin, R. Emparan, C. V. Johnson and R. C. Myers, *Phys. Rev. D* **60**, 064018 (1999).
- [21] A. Chamblin, R. Emparan, C. V. Johnson and R. C. Myers, *Phys. Rev. D* **60**, 104026 (1999).
- [22] C. Niu, Y. Tian and X. N. Wu, *Phys. Rev. D* **85**, 024017 (2012).
- [23] A. Sahay, T. Sarkar and G. Sengupta, *JHEP* **04**, 118 (2010).
- [24] A. Sahay, T. Sarkar and G. Sengupta, *JHEP* **07**, 082 (2010).
- [25] D. Kubiznak, R. B. Mann, *JHEP* **1207**, 033 (2012).
- [26] D. Kastor, S. Ray and J. Traschen, *Class. Quant. Grav.* **26**, 195011 (2009).
- [27] B. P. Dolan, *Class. Quant. Grav.* **28**, 125020 (2011).
- [28] B. P. Dolan, *Class. Quant. Grav.* **28**, 235017 (2011).
- [29] G. 't Hooft, *Conf. Proc. C* **930308**, 284 (1993).
- [30] L. Susskind, *J. Math. Phys.* **36**, 6377 (1995).
- [31] C. Tsallis and L. J. L. Cirto, *Eur. Phys. J. C* **73**, 2487 (2013).
- [32] H. Quevedo, M. N. Quevedo and A. Sanchez, *Eur. Phys. J. C* **79**, 229 (2019).
- [33] C. Tsallis, *J. Statist. Phys.* **52**, 479 (1988).
- [34] J. D. Barrow, *Phys. Lett. B* **808**, 135643 (2020).
- [35] S. Nojiri, S. D. Odintsov and V. Faraoni, *Phys. Rev. D* **105**, 044042 (2022).
- [36] A. Rényi, *Acta Math. Acad. Sci. Hung.* **10**, 193 (1959).
- [37] B. D. Sharma and D. P. Mittal, *J. Comb. Inf. Syst. Sci.* **2**, 122 (1977).
- [38] E. N. Saridakis, *Phys. Rev. D* **102**, 123525 (2020).
- [39] E. N. Saridakis, K. Bamba, R. Myrzakulov and F. K. Anagnostopoulos, *JCAP* **12**, 012 (2018).
- [40] M. Tavayef, A. Sheykhi, K. Bamba and H. Moradpour, *Phys. Lett. B* **781**, 195 (2018).
- [41] G. G. Luciano, *Phys. Rev. D* **106**, 083530 (2022).
- [42] G. G. Luciano, *Phys. Lett. B* **838**, 137721 (2023).
- [43] A. Sheykhi and B. Farsi, *Eur. Phys. J. C* **82**, 1111 (2022).
- [44] H. Shababi and K. Ourabah, *Eur. Phys. J. Plus* **135**, 697 (2020).
- [45] G. G. Luciano, *Eur. Phys. J. C* **81**, 672 (2021).
- [46] G. G. Luciano and M. Blasone, *Phys. Rev. D* **104**, 045004 (2021).
- [47] P. Jizba and G. Lambiase, *Eur. Phys. J. C* **82**, 1123 (2022).
- [48] G. Kaniadakis, *Physica A* **296**, 405 (2001).
- [49] G. Kaniadakis, *Phys. Rev. E* **66**, 056125 (2002).
- [50] G. Kaniadakis, *Phys. Rev. E* **72**, 036108 (2005).
- [51] G. Kaniadakis, M. Lissia and A. M. Scarfone, *Phys. Rev. E* **71**, 046128 (2005).
- [52] G. Kaniadakis, P. Quarati and A. M. Scarfone, *Physica* **305**, 76 (2002).
- [53] G. G. Luciano, *Entropy* **24**, 1712 (2022).
- [54] H. Moradpour, A.H. Ziaie, M. Kord Zangeneh, *Eur. Phys. J. C* **80**, 732 (2020).
- [55] A. Lymperis, S. Basilakos and E. N. Saridakis, *Eur. Phys. J. C* **81**, 1037 (2021).
- [56] N. Drepanou, A. Lymperis, E. N. Saridakis and K. Yesmakhanova, *Eur. Phys. J. C* **82**, 449 (2022).
- [57] A. Sheykhi, [arXiv:2302.13012 [gr-qc]].
- [58] A. Hernández-Almada, G. Leon, J. Magaña, M. A. García-Aspeitia, V. Motta, E. N. Saridakis and K. Yesmakhanova, *Mon. Not. Roy. Astron. Soc.* **511**, 4147 (2022).
- [59] A. Hernández-Almada, G. Leon, J. Magaña, M. A. García-Aspeitia, V. Motta, E. N. Saridakis, K. Yesmakhanova and A. D. Millano, *Mon. Not. Roy. Astron. Soc.* **512**, 5122 (2022).
- [60] G. Lambiase, G. G. Luciano and A. Sheykhi, [arXiv:2307.04027 [gr-qc]].
- [61] I. Cimidiker, M. P. Dabrowski and H. Gohar, *Class. Quant. Grav.* **40**, 145001 (2023).
- [62] A. Kempf, G. Mangano and R. B. Mann, *Phys. Rev. D* **52**, 1108 (1995).
- [63] L. Buoninfante, G. G. Luciano, L. Petruzzello and F. Scardigli, *Phys. Lett. B* **824**, 136818 (2022).
- [64] T. S. Biró and V. G. Czinner, *Phys. Lett. B* **726**, 861 (2013).
- [65] V. G. Czinner and H. Iguchi, *Eur. Phys. J. C* **77**, 892 (2017).
- [66] S. Ghaffari, H. Moradpour, A. H. Ziaie, F. Asghariyan, F. Feleppa and M. Tavayef, *Gen. Rel. Grav.* **51**, 93 (2019).
- [67] H. Moradpour, A. H. Ziaie and C. Corda, *EPL* **134**, 20003 (2021).
- [68] H. Moradpour, A. H. Ziaie, I. P. Lobo, J. P. Morais Graça, U. K. Sharma and A. S. Jahromi, *Mod. Phys. Lett. A* **37**, 2250076 (2022).
- [69] S. Nojiri, S. D. Odintsov and V. Faraoni, *Phys. Rev. D* **104**, 084030 (2021).
- [70] S. Nojiri, S. D. Odintsov and V. Faraoni, *Int. J. Geom. Meth. Mod. Phys.* **19**, 2250210 (2022).
- [71] N. Goldenfeld, *Lectures on phase transitions and the*

- renormalization group*, Westview Press (1992).
- [72] H. J. Reissner, *Annalen Phys.* **50**, 106 (1916).
- [73] E. N. Saridakis, *JCAP* **07**, 031 (2020).
- [74] S. Rani, A. Jawad, H. Moradpour and A. Tanveer, *Eur. Phys. J. C* **82**, 713 (2022).
- [75] A. Jawad and S. R. Fatima, *Nucl. Phys. B* **976**, 115697 (2022).
- [76] G. G. Luciano and A. Sheykhi, [arXiv:2304.11006 [hep-th]].
- [77] S. Basilakos, A. Lymperis, M. Petronikolou and E. N. Saridakis, [arXiv:2308.01200 [gr-qc]].
- [78] G. G. Luciano, *Eur. Phys. J. C* **82**, 314 (2022).
- [79] E. M. C. Abreu and J. A. Neto, *Phys. Lett. B* **835**, 137565 (2022).
- [80] S. Soroushfar and S. Upadhyay, *Phys. Lett. B* **804**, 135360 (2020).
- [81] C. H. Nam, *Eur. Phys. J. C* **78**, 1016 (2018).
- [82] G. A. Marks, F. Simovic and R. B. Mann, *Phys. Rev. D* **104**, 104056 (2021).
- [83] G. M. Deng, J. Fan, X. Li and Y. C. Huang, *Int. J. Mod. Phys. A* **33**, 1850022 (2018).
- [84] A. Alonso-Serrano, M. P. Dabrowski and H. Gohar, *Phys. Rev. D* **103**, 026021 (2021).
- [85] A. Alonso-Serrano, M. P. Dabrowski and H. Gohar, *Int. J. Mod. Phys. D* **27**, 1847028 (2018).
- [86] Z. W. Feng, X. Zhou, S. Q. Zhou and D. D. Feng, *Annals Phys.* **416**, 168144 (2020).
- [87] J. y. Shen, R. G. Cai, B. Wang and R. K. Su, *Int. J. Mod. Phys. A* **22**, 11 (2007).
- [88] R. Mrugala, *Physica* **125A**, 631 (1984).
- [89] P. T. Landsberg and V. Vedral, *Phys. Lett. A* **247**, 211 (1998).
- [90] J. L. Jing, H. W. Yu and Y. J. Wang, *Phys. Lett. A* **178**, 59 (1993).
- [91] H. W. Yu, *Nucl. Phys. B* **430**, 427 (1994).
- [92] X. z. Li and J. g. Hao, *Phys. Rev. D* **66**, 107701 (2002).
- [93] Q. Q. Jiang and S. Q. Wu, *Phys. Lett. B* **635**, 151-155 (2006) [erratum: *Phys. Lett. B* **639**, 684-684 (2006)].
- [94] T. R. P. Caramês, J. C. Fabris, E. R. Bezerra de Mello and H. Belich, *Eur. Phys. J. C* **77**, 496 (2017).
- [95] T. Papanikolaou, A. Lymperis, S. Lola and E. N. Saridakis, *JCAP* **03**, 003 (2023).
- [96] S. Basilakos, D. V. Nanopoulos, T. Papanikolaou, E. N. Saridakis and C. Tzerefos, [arXiv:2307.08601 [hep-th]].
- [97] S. Mignemi, *Mod. Phys. Lett. A* **25**, 1697 (2010).
- [98] J. Giné and G. G. Luciano, *Eur. Phys. J. C* **80**, 1039 (2020).